Available online at www.sciencedirect.com
ScienceDirect
Bioorganic & Medicinal Chemistry Letters 18 (2008) 2355–2361
Bioorganic & Medicinal Chemistry Letters

Design and synthesis of a pyrido[2,3-*d*]pyrimidin-5-one class of anti-inflammatory FMS inhibitors

Hui Huang, Daniel A. Hutta, Huaping Hu, Renee L. DesJarlais, Carsten Schubert, Ioanna P. Petrounia, Margery A. Chaikin, Carl L. Manthey and Mark R. Player*

Johnson & Johnson Pharmaceutical Research & Development, Welsh & McKean Roads, Spring House, PA 19477, USA

Received 23 January 2008; revised 26 February 2008; accepted 27 February 2008
Available online 4 March 2008

Abstract—A series of pyrimidinopyridones has been designed, synthesized and shown to be potent and selective inhibitors of the FMS tyrosine kinase. Introduction of an amide substituent at the 6-position of the pyridone core resulted in a significant potency increase. Compound **24** effectively inhibited in vivo LPS-induced TNF in mice greater than 80%.

Increased tumor-associated macrophage numbers have been associated with tumor progression.[1] In addition, macrophage numbers present within target tissues have been strongly correlated with disease severity in rheumatoid arthritis,[2] and immune nephritis.[3] In some solid tumors, such as breast cancer, elevated macrophage numbers are thought to contribute to disease progression and poor survivability.[4–6] The proliferation and survival of macrophages, monocytes, and their progenitors are driven by macrophage colony-stimulating factor (M-CSF or CSF-1).[7] Binding of CSF-1 to its exclusive receptor, colony-stimulating factor-1 receptor (FMS), induces receptor dimerization and autophosphorylation which leads to the phosphorylation of downstream signaling proteins, and the subsequent differentiation and activation of cells in the macrophage lineage.[8] Animal studies with CSF-1 deficient mice suggest that CSF-1/FMS is a crucial component of a positive cycle that drives chronic inflammation.[9–11] Thus, the inhibition of FMS has great potential in treating human diseases such as rheumatoid arthritis as well as certain cancers where macrophages are pathogenic.

By screening a focused kinase library using Thermofluor® technology,[12] pteridinone **1** was identified as a confirmed hit with an IC_{50} of 0.18 μM for FMS (Fig. 1). A small set of these pteridinones was synthesized and it was observed that replacement of the N-8 phenyl of **1** with an indan ring resulted in a 10-fold potency increase (data not shown).

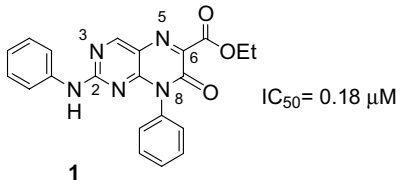

1

Figure 1. High-throughput screening hit **1**.

Compound **1** was modeled in FMS (PDB ID: 2i0y)[13] in order to evaluate the interactions required for binding (Fig. 2). Related pyrido[2,3-*d*]pyrimidin-7-one kinase inhibitors have previously been shown to interact with the hinge region via hydrogen bonds to the amino NH and N-3 of the pyrimidine ring.[14] The model was built assuming similar interactions for the amino NH and the pteridinone N-3 of hit **1** with, respectively, the backbone carbonyl and backbone NH of the hinge residue Cys666. In addition, the following interactions were predicted by this model: a hydrogen bond between the side-chain hydroxyl of Thr663 and the pteridinone N-5, a hydrogen bond between either the pteridinone carbonyl or the ester carbonyl and the terminal amine of Lys616 (depending on side chain conformation), and hydrophobic interactions for the N-8 phenyl.

Keywords: FMS; cFMS; Colony-stimulating factor-1 receptor; CSF-1; M-CSF; Macrophage; Pyrimidinopyridone.
* Corresponding author. Tel.: +1 610 458 6980; fax: +1 610 458 8258; e-mail: mplayer@prdus.jnj.com

0960-894X/$ - see front matter © 2008 Elsevier Ltd. All rights reserved.
doi:10.1016/j.bmcl.2008.02.070

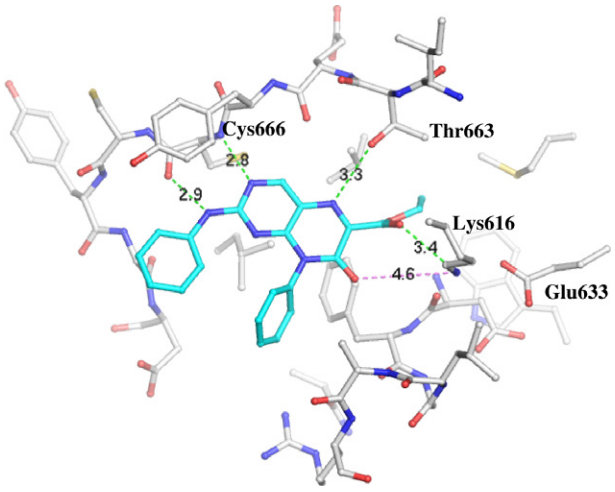

Figure 2. Model of **1** (cyan carbons) in FMS kinase (white carbons). Hydrogen bonds and potential hydrogen bonds are shown as green and magenta dotted lines, respectively.

Based on this model of pteridinone binding, novel scaffolds were explored in an attempt to improve potency. One of the most promising designs was constructed from a 5,8-dihydro-pyrido[2,3-*d*]pyrimidin-5-one scaffold. Represented by **2** (Fig. 3), this scaffold was predicted to bind with a minimal shift of the ring system away from Thr663. With an IC_{50} of 0.25 μM for FMS, **2** showed a 10-fold potency loss compared to its pteridinone analogue (IC_{50} = 0.02 μM). A detailed SAR study was then conducted to improve its in vitro potency. Herein, the structure–activity relationships at three areas of the new scaffold are reported: the C-6 carboxylate ester, N-8 hydrophobic substitution and C-2 anilino substitution.

A linear synthetic method was developed to quickly synthesize analogues of **2** (Scheme 1). An amine, for example, indan-5-ylamine, was reacted with ethyl 3-chloropropionate at elevated temperature in the presence of an inorganic base and a catalytic amount of tetrabutylammonium bromide to afford the aminopropionate ester **3**, which was treated with ethyl 4-chloro-2-methylthio-5-pyrimidinecarboxylate to produce the 4-substituted aminopyrimidine **4**. Cyclization of this diester under Dieckmann conditions afforded bicyclic compound **5**. Subsequent halogenation with bromine followed by dehydrohalogenation gave **6**.[15] The thiomethyl moiety was oxidized to the sulfone **7**, which was subsequently displaced with an amine or aniline by nucleophilic substitution. The resulting carboxylate ester **2** was converted to the carboxylic acid **8** by hydrolysis, or to the amides **9** and **11**–**34** by reaction with the corresponding amines in methanol in a pressure bottle.

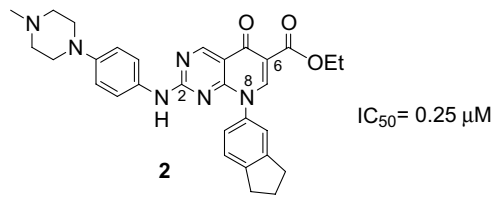

Figure 3. A novel 5,8-dihydro-pyrido[2,3-*d*]pyrimidin-5-one scaffold represented by **2**.

Compound **10**, where N-1 was replaced with CH, was synthesized by the methods shown in Scheme 2. 4,6-Dihydroxynicotinic acid ethyl ester **35** was obtained in two steps from diethyl 1,3-acetonedicarboxylate.[16] Treatment of **35** with phosphorous oxychloride gave 4,6-dichloronicotinic acid ethyl ester **36**. The subsequent nucleophilic displacement yielding **37** and Dieckmann cyclization followed by halogenation/dehydrohalogenation which yielded **38** were similar to the methods outlined in Scheme 1. Substitution of the 2-position chloride of **38** with the piperazinyl aniline was carried out under microwave conditions to afford ethyl ester **39**, which was then converted to the amide **10** by treatment with methanolic ammonia.

All compounds were tested in an in vitro enzyme assay for their abilities to inhibit ATP-induced auto-phosphorylation of FMS (Tables 1 and 2).[17] The most potent compounds were also tested in a functional assay, which was based upon inhibition of CSF-1 driven proliferation of bone marrow-derived macrophages (BMDM).[18] In this cell-based assay, compound **2** was moderately active with an IC_{50} value of 0.47 μM. According to the model, the C-2 anilino substituents are largely solvent-exposed. It seemed likely that the C-6 carboxylate ester and N-8 hydrophobic substitutions would be more important in terms of binding at the active site due to their more intimate contact with the protein. Thus, the C-2 substitution was initially fixed as 4-(4-methyl-piperazin-1-yl)-phenylamine, while the C-6 and N-8 positions were explored (Table 1). The C-6 carboxylic acid **8** was about fourfold less active, whereas transformation of the ester to primary amide **9** resulted in a significant increase in potency. The model of **9** in FMS suggested that the amide could make an intramolecular hydrogen bond to the C-5 carbonyl stabilizing a conformation of the molecule that optimizes hydrogen bonding between the amide carbonyl and the terminal amine of Lys616. The model does not predict that N-1 of the pyrimidine ring is making a direct interaction with FMS. However, removal of N-1 as in **10** decreased potency about fourfold. The greater potency of **9** is likely due to the lower basicity of the aminopyrimidine system, which favors the neutral form of the molecule necessary for interaction with Cys666.

Small alkyl substitution on the C-6 amide was well tolerated, though activity diminished with increasing size of the alkyl group (**11**, **12**). The N-8 substituents occupy a hydrophobic pocket of the active site. Whereas aliphatic rings (**13**–**15**) maintained activity, the unsubstituted phenyl compound **16** significantly attenuated potency. This trend also had been observed within the pteridinone high-throughput screening hit series. Benzylic substitution (**17**) also resulted in a potency decrease, although to a lesser extent than phenyl substitution.

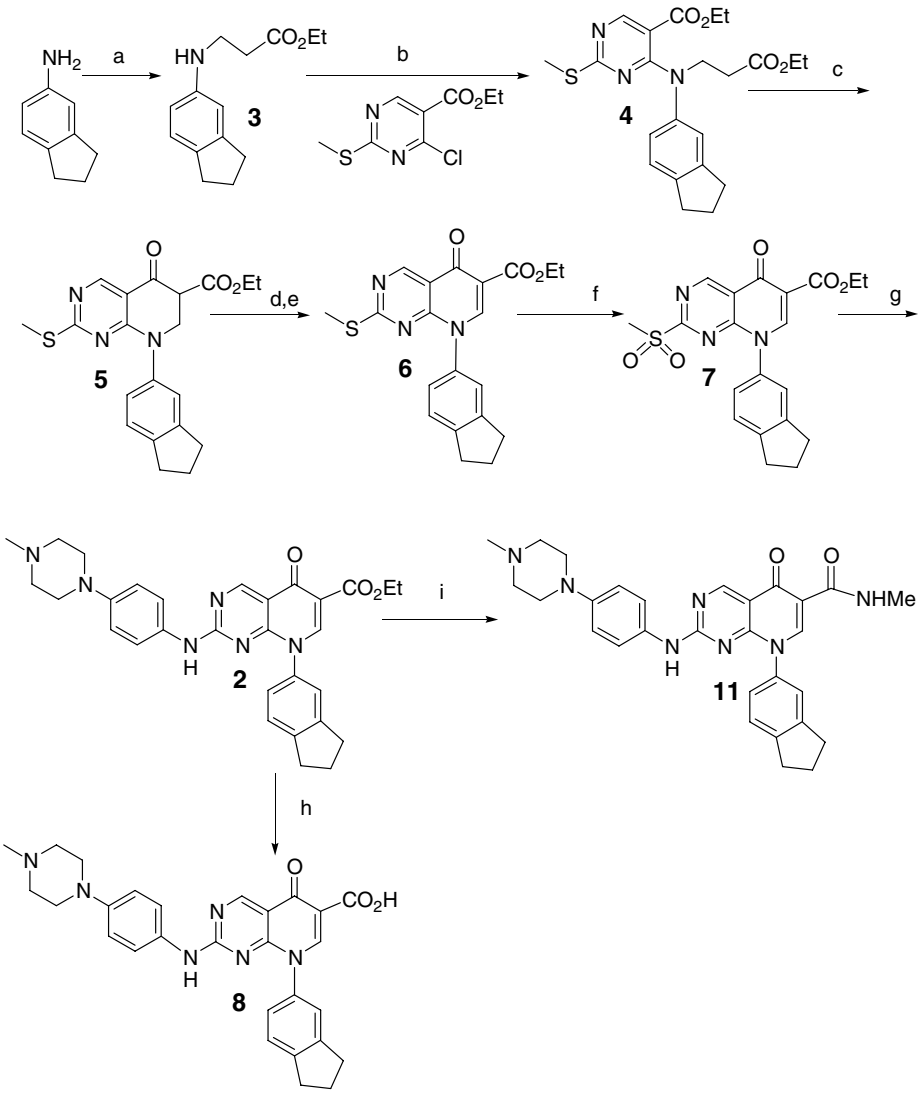

Scheme 1. Reagents and conditions: (a) Ethyl 3-chloropropionate, K_2CO_3, Bu_4NBr (cat.), 100 °C, 71%; (b) Et_3N, *n*-BuOH, rt, 90%; (c) *t*-BuONa, toluene, 90 °C, 62%; (d) Br_2, CH_2Cl_2, rt; (e) Et_3N, CH_2Cl_2, rt, 94%; (f) *m*-CPBA, CH_2Cl_2, rt, 67%; (g) 4-(4-methyl-piperazin-1-yl)-phenylamine, *i*-PrOH, 90 °C, 61%; (h) NaOH, THF, 50 °C, 60%; (i) methylamine, MeOH, rt or 70 °C.

The model predicts that the C-2 anilino NH hydrogen bonds to the protein backbone and the phenyl ring occupies a narrow hydrophobic pocket. Although the substituents at the para or meta positions of the aniline ring are predicted to be solvent-exposed, they did have an effect on activity, as was demonstrated by the potency loss of **18** versus **9**. In addition, this region provided a solubilizing handle for the chemotype. There were no protein backbone contacts in this solvent-exposed region which could adequately explain the changes in potency afforded by different polar substitutions on the aniline ring. Therefore, an extensive search for an optimal C-2 substituent was carried out with C-6 fixed as a primary amide and N-8 as indan (Table 2).

Excellent activity was observed among the 3- or 4-substituted aniline analogues (**9**, **19**–**31**) in both the in vitro enzyme and the BMDM assays. With a 2-hydroxyl substitution, **22** showed a slight potency decline relative to **9**. Introduction of small alkyl linkers between the 4-methylpiperazine and the phenyl ring did not affect the inhibitory activity (**9**, **24** and **25**), although the microsomal stability of the compounds was impacted. With a one-carbon linker, **24** was the least stable compound among the three in both rat liver microsomes (RLMs) and human liver microsomes (HLMs) (Table 3). The same trend was observed with morpholino (**26**, **27**) and dimethylamino analogues (**28**, **29**). Small modifications of the piperazine ring (**19**–**21**, **23**) had little influence on the activity. The compounds with neutral substituents (**30**, **31**) showed similar activities as those with basic ones, but had poorer solubility. When the C-2 substituents were derived from aliphatic amines (**32**–**34**) as opposed to anilines, the activities markedly diminished. This is probably due to the narrow-binding pocket geometry that is better accommodated by flat planar groups.

Because of its excellent BMDM activity, the binding mode of **20** was analyzed using X-ray crystallography.

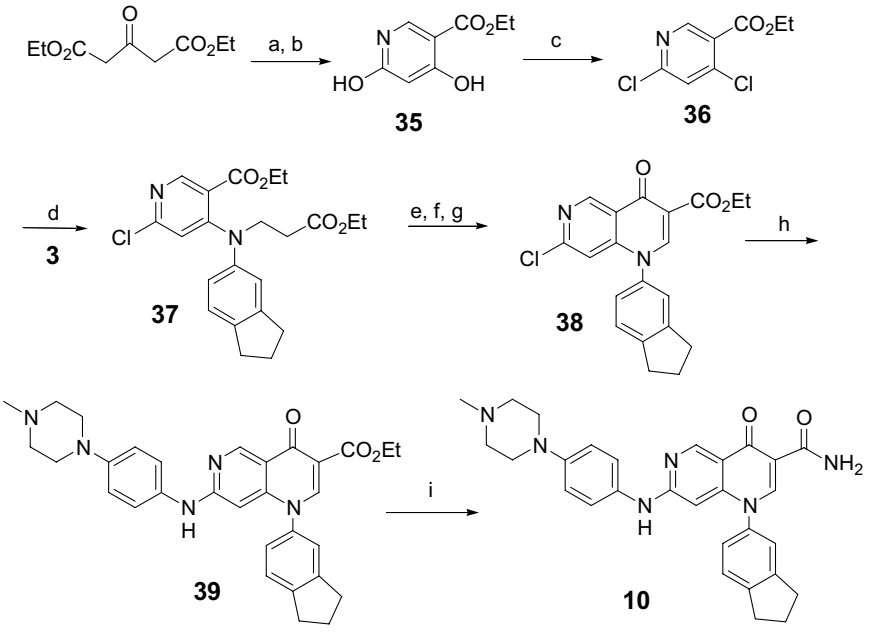

Scheme 2. Reagents and conditions: (a) Trimethylorthoformate, Ac_2O, 120 °C; (b) NH_4OH, rt; (c) $POCl_3$, 100 °C, 68%; (d) Et_3N, DMF, 100 °C, 44%; (e) *t*-BuONa, toluene, 90 °C; (f) Br_2, CH_2Cl_2, rt; (g) Et_3N, CH_2Cl_2, rt, 34%; (h) 4-(4-methyl-piperazin-1-yl)-phenylamine, Et_3N, NMP, microwave irradiation, 200 °C, 18%; (i) NH_3, MeOH, rt, 65%.

Table 1. 6- and 8-Position modifications to the 5,8-dihydro-pyrido[2,3-*d*]pyrimidin-5-one series

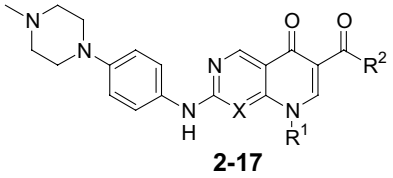

2-17

Compound	X	R^1	R^2	Auto-P_i IC_{50}[a] (μM)	BMDM IC_{50}[b] (μM)
2	N	Indan-5-yl	OEt	0.25	0.47
8	N	Indan-5-yl	OH	1.1	ND
9	N	Indan-5-yl	NH_2	0.013	0.016
10	C	Indan-5-yl	NH_2	0.056	ND
11	N	Indan-5-yl	NHMe	0.031	ND
12	N	Indan-5-yl	NHEt	0.068	ND
13	N	Cyclohexyl	NH_2	0.035	ND
14	N	Cyclopentyl	NH_2	0.056	ND
15	N	Bicyclo[2.2.1]hept-2-yl	NH_2	0.081	ND
16	N	Phenyl	NH_2	0.73	ND
17	N	Benzyl	NHMe	0.42	ND

[a] Reported IC_{50} values are means of three experiments. Inter-assay variance was <10%.
[b] Dose–response data are the average of at least two replicates per dose.

Like all previously analyzed FMS inhibitors,[19] **20** is located in the ATP binding pocket (Fig. 4A). Consistent with the aforementioned model, this series interacts with the hinge region of the kinase via crucial hydrogen-bonding interactions mediated through the C-2 amino NH and the pyrimidine N-3 (Fig. 4). Like the N-5 of the pteridinones, the C-5 carbonyl oxygen of the 5,8-dihydro-pyrido[2,3-*d*]pyrimidin-5-one forms a hydrogen bond with the hydroxyl group of Thr663.

Since the oxygen and NH of the terminal amide share the same number of electrons, their position cannot be distinguished by crystallographic means. However, based on an analysis of the hydrogen-bonding patterns for both rotamers of the amide, the depicted rotamer is proposed to be the favored orientation. Here the amide is engaged in an intramolecular hydrogen bond with the C-5 carbonyl oxygen (Fig. 4, magenta), thereby stabilizing a flat conformation of the pyrimidinopyridone core and positioning the amide carbonyl for its interaction with Lys616. Furthermore, the amide-nitrogen is also part of a water-mediated hydrogen-bonding network, which includes the hydroxyl group of Thr663, the C-5 carbonyl oxygen and two water mole-

Table 2. 2-Position modifications to the 5,8-dihydro-pyrido[2,3-*d*]pyrimidin-5-one series

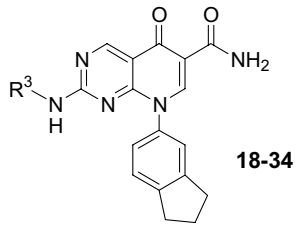

Compound	R^3	Auto-P_i IC_{50}[a] (μM)	BMDM IC_{50}[b] (μM)
18	Phenyl	0.28	ND
9	4-(4-Methyl-piperazin-1-yl)-phenyl	0.013	0.016
19	4-Piperazin-1-yl-phenyl	0.005	0.004
20	4-(3,5-Dimethyl-piperazin-1-yl)-phenyl	0.007	0.003
21	3-(4-Methyl-piperazin-1-yl)-phenyl	0.008	0.006
22	2-Hydroxy-4-(4-methyl-piperazin-1-yl)-phenyl	0.093	ND
23	4-Piperidin-4-yl-phenyl	0.008	0.051
24	4-(4-Methyl-piperazin-1-ylmethyl)-phenyl	0.014	0.011
25	4-[2-(4-Methyl-piperazin-1-yl)-ethyl]-phenyl	0.008	0.009
26	4-Morpholin-4-ylmethyl-phenyl	0.022	0.027
27	4-(2-Morpholin-4-yl-ethyl)-phenyl	0.008	0.008
28	4-Dimethylaminomethyl-phenyl	0.021	0.004
29	4-Dimethylaminoethyl-phenyl	0.003	0.016
30	3-(Piperidin-1-yl-methanone)phenyl	0.004	0.014
31	*S*-4-[4-(Oxazolidin-2-one)-methyl]-phenyl	0.012	0.09
32	2-Morpholin-4-yl-ethyl	3.3	ND
33	3-(4-Methyl-piperazin-1-yl)-propyl	1.8	ND
34	3-Imidazol-1-yl-propyl	2.3	ND

[a] Reported IC_{50} values are means of three experiments. Inter-assay variance was <10%.
[b] Dose–response data are the average of at least two replicates per dose.

cules present in close proximity. The co-crystal structure confirmed the modeling predictions and provided the structural basis for further lead optimization within this series.

FMS is a member of the type III receptor tyrosine kinases that also includes FLT-3, PDGFR-β and KIT. Table 4 shows the kinase selectivity of compound **9** and **24**. Both are potent inhibitors of FLT-3 and KIT, but highly selective over PDGFR-β, Axl, IRK-β and Src. They inhibited the neurotrophic type I tyrosine kinase receptor, TrkA with modest potency. To further evaluate specificity, compound **9** and **24** were assessed in a standard counterscreening panel of fifty receptors, transporters and ion channels (data not shown). At a concentration of 5 μM, **9** inhibited human A3 binding at 55% with no other assays showing greater than 50% inhibition. In the case of **24**, only two assays indicated inhibition of control-specific binding greater than 50% at a concentration of 10 μM. These were human A2A and A3 with 60% and 58% inhibition, respectively.

Table 3. The effect of alkyl chain length on microsomal stability

Compound	HLM[a]	RLM[a]
9	80.5	87.3
24	74	54
25	96	84
26	2.5	9.7
27	58	83
28	35	38
29	88	65

[a] Percent remaining 10 min after incubating the compounds with liver microsomes.

Due to their desirable in vitro properties, compound **9** and **24** were profiled for their pharmacokinetic (PK) properties in the rat. After an intravenous injection at 2 mg/kg, **9** showed very high clearance (CL = 133 mL/min/kg) and a high volume of distribution (V_d = 18.7 L/kg). After an oral dose of 10 mg/kg, the plasma concentrations of **9** were below detectable levels. The PK profile of **24** was not significantly improved, with high clearance (CL = 29 mL/min/kg) and high volume of distribution (V_d = 26.5 L/kg). Compound **24** exhibited low oral bioavailability (4%).

Administration of FMS inhibitors was shown previously to inhibit LPS-induced TNFα in mice.[20] To examine the in vivo activity of **24**, groups of eight male Swiss Webster mice were administered vehicle (20% hydroxpropyl-β-cyclodextrin) or **24** at 20 or 50 mg/kg by the intraperitoneal route. Three hours later saline or LPS (100 μg/kg) in saline was administered via the tail vein. TNFα was measured by ELISA (R&D Systems) in plasma harvested by cardiac puncture from mice euthanized 90 min after the LPS dose. Compound **24** at 20 and 50 mg/kg inhibited LPS-induced TNFα by 81% and 87%, respectively (Table 5).

In conclusion, a novel series of 5,8-dihydro-pyrido[2,3-*d*]pyrimidin-5-ones was designed and synthesized as

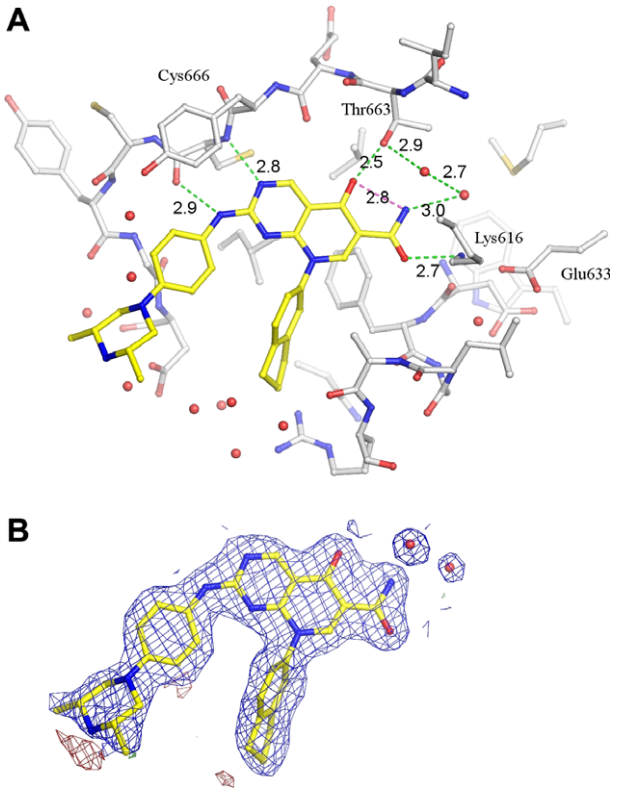

Figure 4. Close-up view of the ligand-binding site. (A) Ball-and-stick representation of **20** (yellow carbons) bound in the active site of FMS (grey carbons). Hydrogen bonds to the backbone of the protein and within the water-network are depicted as green dashed lines and the internal hydrogen-bond between the amide nitrogen and the C5 carbonyl oxygen is drawn in magenta. (B) Ball-and-stick representation of **20** in a $2f_o$-f_c electron density map (blue) contoured at 1.4σ and truncated to a radius of 2 Å beyond each atom for clarity. Also drawn is a f_o-f_c electron density map contoured to 3σ (green) and -3σ (red), truncated beyond 3 Å. (PDB ID: 3BEA).

Table 4. IC_{50} data of compound **9** and **24** in a kinase counterscreen

Kinase	**9**[a] (μM)	**24**[a] (μM)
FMS	0.013	0.014
FLT-3	0.003	0.001
KIT	0.056	0.028
PDGFR-β	>1	>2
Axl	>0.3	>0.5
TrkA	0.2	0.31
IRK-β	>1	>2
Src	1	1.5

[a] IC_{50} values were determined at the respective ATP Km for each kinase.

inhibitors of FMS. Conversion of the C-6 carboxylic ester of **2** to a primary amide as in **9**, led to a significant increase in inhibitory potency. The structural basis for this enhanced activity was provided by the co-crystal structure of **20** in FMS. The exceptional in vitro potency of this series translated into robust in vivo activity of **24** as demonstrated by inhibition of LPS-induced TNFα in mice. Although **24** and **9** suffered from poor oral PK, this series provided novel structural insight into the mechanism of FMS inhibition and serves as a lead series for further optimization.

Table 5. Compound **24** inhibits in vivo LPS-induced TNFα

Pretreatment[a]	Challenge[b]	TNFα[c] (pg/ml)
Vehicle	Saline	12 (5)
Vehicle	LPS	3688 (566)
Compound **24**, 20 mg/kg	LPS	687 (80)*
Compound **24**, 50 mg/kg	LPS	499 (61)*

[a] Mice were predosed by intraperitoneal injection with vehicle or **24** three hours prior to LPS challenge.
[b] Saline or 100 μg/kg LPS (Sigma, 0127:B8) via tail vein.
[c] Mean (SEM) plasma TNFα 90 min after challenge.
* $p < 0.01$ versus vehicle plus LPS.

References and notes

1. Chen, J. J. W.; Lin, Y. C.; Yao, P. L.; Yuan, A.; Chen, H. Y.; Shun, C. T.; Tsai, M. F.; Chen, C. H.; Yang, P. C. *J. Clin. Oncology* **2005**, *23*, 953.
2. Yanni, G.; Whelan, A.; Feighery, C.; Bresnihan, B. *Ann. Rheum. Dis.* **1994**, *53*, 39.
3. (a) Yang, N.; Isbel, N. M.; Nikolic-Paterson, D. J.; Li, Y.; Ye, R.; Atkins, R. C.; Lan, H. Y. *Kidney Int.* **1998**, *54*, 143; (b) Isbel, N. M.; Nikolic-Patterson, D. J.; Hill, P. A.; Dowling, J.; Atkins, R. C. *Nephrol. Dial. Transplant.* **2001**, *16*, 1638.
4. Kluger, H. M.; Dolled-Filhart, M.; Rodov, S.; Kacinski, B. M.; Camp, R. L.; Rimm, D. L. *Clin. Cancer Res.* **2004**, *10*, 173.
5. Lin, E. Y.; Nguyen, A. V.; Russell, R. G.; Pollard, J. W. *J. Exp. Med.* **2001**, *193*, 727.
6. Yee, L. D.; Liu, L. *Anticancer Res.* **2000**, *20*, 4379.
7. Sherr, C. J. *Biochim. Biophys. Acta* **1988**, *948*, 225.
8. (a) Pixley, F. J.; Stanley, E. R. *Trends Cell Biol.* **2004**, *14*, 628; (b) Sherr, C. J.; Roussel, M. F.; Rettenmier, C. W. *J. Cell. Biochem.* **1988**, *38*, 179.
9. Campbell, I. A.; Rich, M. J.; Bischof, R. J.; Hamilton, J. A. *J. Leukocyte Biol.* **2000**, *68*, 144–150.
10. Pollard, J. W.; Stanley, E. R. *Adv. Dev. Biochem.* **1995**, *4*, 153.
11. Van Wesenbeeck, L.; Odgren, P. R.; MacKey, C. A.; D'Angelo, M.; Safadi, F. F.; Popoff, S. N.; Van Hul, W.; Marks, S. C., Jr. *PNAS* **2002**, *99*, 14303.
12. Carver, T. E.; Bordeau, B.; Cummings, M. D.; Petrella, E. C.; Pucci, M. J.; Zawadzke, L. E.; Dougherty, B. A.; Tredup, J. A.; Bryson, J. W.; Yanchunas, J., Jr.; Doyle, M. L.; Witmer, M. R.; Nelen, M. I.; DesJarlais, R. L.; Jaeger, E. P.; Devine, H.; Asel, E. D.; Springer, B. A.; Bone, R.; Salemme, F. R.; Todd, M. J. *J. Biol. Chem.* **2005**, *280*, 11704.
13. Schubert, C.; Schalk-Hihi, C.; Struble, G. T.; Ma, H. C.; Petrounia, I. P.; Brandt, B.; Deckman, I. C.; Patch, R. J.; Player, M. R.; Spurlino, J. C.; Springer, B. A. *J. Biol. Chem.* **2007**, *282*, 4094.
14. Berman, H. M.; Westbrook, J.; Feng, Z.; Gilliland, G.; Bhat, T. N.; Weissig, H.; Shindyalov, I. N.; Bourne, P. E. *Nuc. Acids Res.* **2000**, *28*, 235.
15. Barvian, M.; Boschelli, D. H.; Cossrow, J.; Dobrusin, E.; Fattaey, A.; Fritsch, A.; Fry, D.; Harvey, P.; Keller, P.; Garrett, M.; La, F.; Leopold, W.; McNamara, W.; Quin, M.; Trumpp-Kallmeyer, S.; Toogood, P.; Wu, Z.; Zhang, E. *J. Med. Chem.* **2000**, *43*, 4606.

16. Pesson, M.; Antoine, M.; Chabassier, S.; Geiger, S.; Girard, P.; Richer, D.; De Lajudie, P.; Horvath, E.; Leriche, B.; Patte, S. *Eur. J. Med. Chem.* **1974**, *9*, 585.
17. Ruesdale, L. K.; Sherbine, J. P.; Vanasse, B. J. *PCT Int. Appl.* **(1997), WO9724327A1.**
18. Schalk-Hihi, C.; Ma, H. C.; Struble, G. T.; Bayoumy, S.; Williams, R.; Devine, E.; Petrounia, I. P.; Mezzasalma, T.; Zeng, L.; Schubert, C.; Grasberger, B.; Springer, B. A.; Deckman, I. C. *J. Biol. Chem.* **2007**, *282*, 4085.
19. Patch, R. J.; Brandt, B. M.; Asgari, D.; Baindur, N.; Chadha, N. K.; Georgiadis, T.; Cheung, W. S.; Petrounia, I. P.; Donatelli, R. R.; Chaikin, M. A.; Player, M. R. *Bioorg. Med. Chem. Lett.* **2007**, *17*, 6070.
20. Conway, J. G.; McDonald, B.; Parham, J.; Keith, B.; Rusnak, D. W.; Shaw, E.; Jansen, M.; Lin, P.; Payne, A.; Crosby, R. M.; Johnson, J. H.; Frick, L.; Lin, M. H. J.; Depee, S.; Tadepalli, S.; Votta, B.; James, I.; Fuller, K.; Chambers, T. J.; Kull, C. K. *Proc. Natl. Acad. Sci.* **2005**, *102*, 16078.